Materials Today Communications 28 (2021) 102721

Contents lists available at ScienceDirect

Materials Today Communications

journal homepage: www.elsevier.com/locate/mtcomm

New bio-based sustainable polymers and polymer composites based on methacrylate derivatives of furfural, solketal and lactic acid☆

Raynold Techie-Menson [a], Charles K. Rono [a], Anita Etale [b], Gift Mehlana [c], James Darkwa [a], Banothile C.E. Makhubela [a,*]

[a] Research Centre for Synthesis and Catalysis, Department of Chemical Sciences, University of Johannesburg, Auckland Park, 2006 Johannesburg, South Africa
[b] Molecular Sciences Institute, School of Chemistry, University of the Witwatersrand, Johannesburg, South Africa
[c] Department of Chemical Technology, Faculty of Science and Technology, Midlands State University, 9055 Senga Road, Gweru, Zimbabwe

ARTICLE INFO

Keywords:
Bio-based
Furfural
Glycerol
Lactic acid
Polyacrylate
Renewable
Sustainable

ABSTRACT

Monomers derived from renewable sources are of great interest to drive sustainable polymer chemistry. Herein, bio-based furfural, glycerol and lactic acid were used as building blocks to prepare methacrylate monomers via simple transesterification reactions in high yield and purity. The monomers were polymerized and co-polymerized by employing a free radical solution polymerization technique using 1,1-azobis cyclohexanecarbonitrile (ABCN) initiator. The resultant new co-polymers (P(FAMA-co-SoMA), P(FAMA-co-LAMA) and P(SoMA-co-LAMA)) were obtained in high yields and proved to have sizeable molecular weights (M_w from 2540 to 29395 g mol^{-1} and M_n from 2194 to 7463 $gmol^{-1}$). Thermogravimetric analysis and differential scanning calorimetry (DSC) measurements on these polymers revealed good thermal properties (thermal stability ranging between 125 °C and 155 °C) with some crystalline regions identified by DCS and PXRD. The polymers were reinforced using cellulose triacetate and polysulfone to give new polymer composites (Psf/PFAMA, Psf/PFAMA-co-SoMA, Psf/PSoMA, CTA/PFAMA, CTA/PFAMA-co-SoMA, CTA/PSoMA), which were amorphous and degraded hydrolytically (in acidic and basic aqueous solutions) by up to 10% in just 24 h. The polymer composites were fashioned into thin films and membranes and applied preliminarily as coatings and water filtration membranes.

1. Introduction

The synthesis of sustainable monomers and polymers from renewable resources is a topic of intense research, mainly because of the carbon footprint and environmental degradation associated with processing and producing fossil-based monomers and polymers. Presently, the manufacture of polymers from fossil resources accounts for about 7% [1] of global oil and gas usage and will probably increase significantly unless alternate sustainable sources of monomers are developed [2]. Processing fossil feedstock to produce monomers and polymers often consumes a lot of energy and results in high emissions of earth-warming greenhouse gases [1]. Also, most polymers presently used widely in packaging, elastomers, coatings, electronic, industrial and construction parts, etc., are designed to be resistant to degradation. This means that these polymers lead to further pollution of the environment at the end of their use if not disposed of correctly.

A recent report shows that society may have more polymer waste than fish in the oceans in thirty years due to the increase in polymer waste [3]. Therefore, using traditional fossil-based feedstocks to make monomers that generate polymers that degrade slowly needs to be averted for biogenic or sustainable polymers. These sustainable polymers need to have equal or better performance than fossil-based counterparts and break down easily in the environment either by hydrolysis, photolytically or through microorganisms [4].

The perceived high cost and poor performance of biodegradable or sustainable polymers relative to fossil-based polymers have led to little progress in the global polymer market share (which stands at <5% of biodegradable polymers) [1]. If there is to be a notable shift favouring sustainable polymers, creative synthetic procedures from renewable feedstocks are needed. These should be inexpensive, scalable and easy to adopt [1]. Monomers like terpenes, fatty acids from vegetable oils, carbohydrates, and carbon dioxide can be utilized as raw materials to

☆ We dedicate this work to the memory of Novisi K. Oklu

* Corresponding author.
E-mail address: bmakhubela@uj.ac.za (B.C.E. Makhubela).

https://doi.org/10.1016/j.mtcomm.2021.102721
Received 17 May 2021; Received in revised form 10 August 2021; Accepted 12 August 2021
Available online 24 August 2021

produce diverse sustainable materials and products, including elastomers, plastics, hydrogels, flexible electronics, resins, engineering polymers and composites [5,6].

Among the biomass fractions, lignocellulose (comprising cellulose, hemicellulose and lignin) is known to be the most abundant resources on the planet [7]. Pretreatment of lignocellulosic biomass yields cellulose, hemicellulose and lignin. The cellulose and hemicellulose components can be hydrolyzed to generate C_5, and C_6 sugars, including mannose, galactose, xylose, arabinose, rhamnose etc [8]. These sugars can further be transformed into important bio-based chemicals, such as furfural (FF) and 2-hydroxymethylfurfural (HMF), lactic acid and glycerol through a selection of fermentation and dehydration processes [9]. Fatty acids, obtained from lipids found in animal fats and vegetable oils, are also an essential source of biomass, which provides hydrocarbons for fuel (e.g. fatty acid methyl esters, FAMEs) and glycerol [10]. Notably, glycerol can also be derived from the fermentation of sugars [11–14]. By employing synthetic methodologies, these biochemicals (FF, HMF, lactic acid and glycerol) can be transformed into monomers [15,16].

Amidst the vast transformation of furfural into valuable chemicals and fuels, the most common ones involve furfuryl alcohol [17,18]. Furfuryl alcohol has an enormous spectrum of utilization, such as in the production of solvents, biofuel(additives) and polymers – the latter requiring pre-modification into monomers [19,20]. A typical example is furfuryl methacrylate (FMA) [21], a useful monomer obtained by the reaction of furfuryl alcohol with methacrylic acid /anhydride generating a radical polymerization handle [22].

Glycerol can also be modified into a monomer with a methacrylate polymerization handle by 1) initial treatment with acetone, under catalytic acetalization to afford solketal [23] then, 2) reaction of the solketal with methacrylic acid/anhydride to give solketal methacrylate [24]. Similarly, lactic acid can be treated with methacrylic acid/-anhydride to afford lactic acid methacrylate [25].

In this work, we report on the synthesis of methacrylate monomers, including furfuryl alcohol-methacrylate (FAMA), solketal-methacrylate (SoMA) and lactic acid-methacrylate (LAMA). Subsequent homo- and co-polymerization by free radical polymerization with 1,1-azobiscyclohexanecarbonitrile (ABCN) as the initiator resulted in new and known bio-based polymers that have been fully characterized. Formation of polymer composites by combining the new co-polymers (P(FAMA-co-SoMA), P(FAMA-co-LAMA) and P(SoMA-co-LAMA)) with some commercially available polymers (cellulose triacetate and polysulfone) produced new composites (Psf/PFAMA, Psf/PFAMA-co-SoMA, Psf/PSoMA, CTA/PFAMA, CTA/PFAMA-co-SoMA, CTA/PSoMA) used as coatings and also fashioned into film membranes for water purification.

2. Experimental

2.1. Materials

Furfural, glycerol (99.5%), formic acid (95%), triethylamine (99%), acetone, Iron(III)chloride hexahydrate ($FeCl_3.6H_2O$), methacrylic anhydride (MAN) (92%), 4-(dimethylamino) pyridine (DMAP) (99%), lactic acid (85%), methacrylic acid (99%), methane sulfonic acid (99.5%), hydroquinone (99%), Polysulfone (Psf), cellulose triacetate (CTA) 1,1- azobis(cyclohexanecarbonitrile) (ABCN), sodium hydrogen bicarbonate ($NaHCO_3$) sodium hydroxide and hydrochloric acid were all purchased from Sigma-Aldrich and were used as supplied. Platinum-based catalyst (**C5**) was available in our laboratory, prepared in a previous work [26], and furfuryl alcohol was prepared as previously reported from our laboratory [26]. Solketal was synthesized following the reported literature method [27]. Furfuryl alcohol methacrylate (FAMA), solketal methacrylate (SoMA) and lactic acid methacrylate (LAMA) monomers were synthesized following the reported literature method [28]. Solvents such as hexane, ethyl acetate, tetrahydrofuran, toluene and chloroform were purchased from Sigma-Aldrich and were used as received.

2.2. Instrumentation

^{1}H NMR (400 MHz) and $^{13}C\{^1H\}$ NMR (100 MHz) spectra were recorded on a Bruker-400 MHz spectrometer, and values were reported relative to tetramethylsilane (δ 0.0) as internal standard. The instrument operated at a temperature of 25 ^oC. All chemical shifts values were recorded in ppm. FT-IR spectra were recorded using a Perkin Elmer FT-IR Spectrum BX-ATR.

Thermogravimetric (TGA) measurements were performed using a Perkin Elmer TGA-DSC SDT Q600 V20.9 Build 20. The samples were heated from 25° to 600 °C at a heating rate of 10 °C min^{-1} under a nitrogen atmosphere in standard aluminium pans (sample weight: 1–10 mg).

Differential scanning calorimetry (DSC) measurements were performed in a Mettler Toledo DSC 822e with a heating rate of 10 °C min^{-1} in aluminium pans (sample weight: 10–20 mg). Samples were scanned from 0° to 400 °C.

Waters 1515 isocratic HPLC pump, a Waters 717plus auto-sampler, Waters 600E system controller (run by Breeze Version 3.30 SPA) and a Waters in-line Degasser AF (SEC), equipped with a Waters 410 differential refractometer and a UV/Vis detector (λ = 254 and 320 nm) with two PLgel (Agilent Technologies) 5 μm Mixed-C (300 ×7.5 mm i.d) columns and a pre-column (PLgel 5 μm Guard, 50 ×7.5 mm i.d) were used to measure the molecular weight of polymers. A series of narrow polystyrene standards ranging from 580 $gmol^{-1}$ to 2 × 10^6 $gmol^{-1}$ were used for calibrations and (THF, HPLC grade, stabilized with 0.125% BHT) with a flow rate of 1 mL min^{-1} at 30 °C was used as the column eluent.

Powder X-ray Diffraction (P-XRD) were recorded on a Panalytical X'Pert X-Ray diffractometer. Diffraction patterns were reported in arbitrary units [a.u.] on the vertical axis and position [2θ (^{o})] on the horizontal axis within a range of 4–90 2θ (^{o}).

Scanning Electron Microscopy (SEM) micrographs were recorded on a Tescan Scanning Electron Microscope equipped with an Oxford INCA Energy Dispersive Spectroscopy (EDAX) detector, using a secondary electron signal and Vega software to capture images.

Transmission Electron Microscopy (TEM) micrographs were recorded on a Jeol Jem-2100 electron microscope coupled with an EDAX.

2.3. Synthesis

2.3.1. Synthesis of furfuryl alcohol methacrylate (FAMA) and solketal methacrylate (SoMA) monomers

FAMA and **SoMA** were prepared according to literature procedures [28,29]. To synthesize **FAMA**, 4-(dimethylamino) pyridine (DMAP) (0.026 g, 0.212 mmol) and triethylamine (TEA) (4 mL, 30.58 mmol) were charged into a 100 mL round bottom flask. Furfuryl alcohol (1.8 mL, 20.39 mmol) was added, followed by 5 mL ethyl acetate. The flask was sealed, and the whole mixture was stirred under nitrogen for 30 min to ensure the formation of a homogenous mixture. Methacrylic anhydride (MAN) (3.2 mL, 21.42 mmol) was mixed with 3 mL of ethyl acetate and added to the mixture dropwise. After the complete addition of MAN, the solution was allowed to stir under nitrogen for about 3 – 4 h, followed by heating at 55 °C for 24 h. After the reaction, the solution was further diluted by adding about 40 mL of ethyl acetate and then transferred into a separatory funnel and washed with three portions of saturated aqueous $NaHCO_3$ solution. The organic layer was then filtered to remove TEA and any other salt formed. The resulting solution was then evaporated and dried under a vacuum to remove ethyl acetate. A brown liquid was then obtained. Yield: 3.05 g, (89%). ^{1}H NMR (400 MHz, $CDCl_3$): δ 1.93 (s, 3 H, H_f), 5.11 (s, 2 H, H_d), 5.55 (s, 1 H, H_{e1}), 6.11 (s, 1 H, H_{e2}), 6.34–6.35 (t, $J_{H\text{-}H}$ = 2.4 Hz, 1 H, H_b), 6.41 (d, $J_{H\text{-}H}$ = 2.4 Hz, 1 H, H_c), 7.41 (d, $J_{H\text{-}H}$ = 0.8 Hz, 1 H, H_a); $^{13}C\{^1H\}$ NMR (100 MHz, $CDCl_3$): δ 18.3(C_9), 58.3 (C_5), 110.5 (C_4), 110.6 (C_3), 126.1 (C_8), 136.0 (C_7), 143.2 (C_2), 149.6 (C_1), 167.1 (C_6). FT-IR (ν_{max}/cm): 1636 (-C═C), 1716 (-C═O).

SoMA was also synthesized following the same reaction procedure for FAMA. 4-(Dimethylamino) pyridine (DMAP) (9.63 mg, 0.079 mmol), triethylamine (TEA) (1.59 mL, 11.36 mmol), Solketal (0.94 mL, 7.57 mmol), Methacrylic anhydride (MAN) (1.23 mL, 8.32 mmol). Yield: 1.35 g, (89%). ^{1}H NMR (400 MHz, $CDCl_3$): δ 1.35 (s, 3 H, H_{d1}), 1.41 (s, 3 H, H_{d2}), 1.93 (t, $J_{H\text{-}H}$ = 1.2 Hz, 3 H, H_f), 3.76 – 3.79 (m, 1 H, H_{c1}), 4.05 – 4.09 (m, 1 H, H_{c2}), 4.17 – 4.19 (q, $J_{H\text{-}H}$ = 0.4 Hz, 2 H, H_a), 4.31 – 4.37 (m, 1 H, H_b), 5.56 – 5.58 (q, $J_{H\text{-}H}$ = 1.6 Hz, 1 H, H_{e1}), 6.12 (t, $J_{H\text{-}H}$ = 0.8 Hz, 1 H, H_{e2}); ^{13}C{^{1}H} NMR (100 MHz, $CDCl_3$): δ 18.3 (C_9), 25.4 (C_{5b}), 26.7 (C_{5a}), 64.7 (C_4), 66.4 (C_3), 73.6 (C_2), 109.8 (C_1), 126.1 (C_8), 135.9 (C_7), 167.1 (C_6). FT-IR (ν_{max}/cm): 1638 (-C═C), 1719 (-C═O).

2.3.2. Synthesis of lactic acid methacrylate monomer (LAMA)

LAMA was prepared according to the literature procedure [25]. Lactic acid (1 g, 0.011 mol) and hydroquinone (0.61 mg, 0.005 mmol) were charged into a 100 mL round bottom flask and heated in an oil bath to a temperature of 100 °C. Methacrylic acid (0.96 g, 0.011 mol) and methane sulfonic acid (0.011 g, 0.11 mmol) were then added dropwise to the reaction mixture. The whole mixture was then stirred and heated at 100 °C for 3 h. A brown liquid was then obtained. Yield: 1.50 g (86%). ^{1}H NMR (400 MHz, $CDCl_3$): δ 1.45–1.57 (m, 3 H, H_d), 1.92–1.95 (m, 3 H, H_c), 4.32 – 4.37 (m, 1 H, H_b), 5.63–5.68 (m, 1 H, H_a), 6.19–6.23 (m, 1 H, H_a); ^{13}C{^{1}H} NMR (100 MHz, $CDCl_3$): δ 17.9 (C_7), 20.2 (C_6), 66.6 (C_5), 128.1 (C_4), 135.6 (C_3), 173.0 (C_2), 180.8 (C_1). FT-IR (ν_{max}/cm): 2500 – 3500 cm^{-1} (-COOH), 1705 cm^{-1} (-C═O), 1628 cm^{-1} (-C═C).

2.3.3. Synthesis of poly(furfuryl alcohol methacrylate) (PFAMA) and poly (solketal methacrylate) (PSoMA) homopolymers

Free radical polymerization of furfuryl alcohol methacrylate (FAMA) was performed using 1,1-azobis(cyclohexanecarbonitrile) (ABCN) as the initiator and toluene as solvent. FAMA (1.00 g, 6.02 mmol) was added into a pre-dried round-bottom flask, and about 5 mL of dried toluene was added to it. Air was removed and replaced with nitrogen using a series of freezing and thawing cycles in a vacuum. The reaction flask was then placed in a preheated oil bath at a temperature of 88 °C with stirring. After 5 min of stirring, ABCN (0.74 g, 3.01 mmol) was dissolved in dried toluene and then added to the mixture. The reaction mixture was then stirred at 88 °C for a maximum of 24 h. After 24 h, tetrahydrofuran was added to the polymer mixture, precipitated in excess hexane and vacuum dried. The dried polymer was then weighed (0.7798 g) and further characterized. ^{1}H NMR (400 MHz, $CDCl_3$): δ 0.85 – 1.76 (b, 5 H, H_e, H_f), 4.88 – 4.97 (b, 2 H, H_d), 6.32 – 6.34 (b, 2 H, H_b, H_c), 7.39 (b, 1 H, H_a); FT-IR (νmax/cm^{-1}): 1716 (-C═O).

PSoMA was also synthesized following the same reaction procedure for PFAMAs. Solketal methacrylate (2.00 g, 9.99 mmol) ABCN (1.22 g , 4.99 mmol). ^{1}H NMR (400 MHz, $CDCl_3$): δ 0.87 – 1.23 (b, 3 H, H_c, H_d, H_e), 1.34 – 1.41 (b, 6 H, H_f, H_g), 1.55 – 2.12 (b, 2 H, H_a,), 3.73 – 4.29 (b, 5 H, H_c, H_d, H_e); FT-IR (ν_{max}/cm): 1719 (-C═O).

2.3.4. Synthesis of lactic acid methacrylate (PLAMA) homopolymer

PLAMA was prepared using the same procedures for PFAMA using LAMA in place of FAMA and ethyl acetate as the solvent. PLAMA gave a mass of 0.25 g. ^{1}H NMR (400 MHz, $CDCl_3$): δ 1.12 – 2.13 (b, 8 H, H_b, H_c, H_d), 4.19 – 4.34 (b, 1 H, H_a); FT-IR (ν_{max}/cm): 1716 (-C═O), 2500 – 3500 cm^{-1} (-COOH).

2.3.5. Synthesis of poly(furfuryl alcohol methacrylate-co-solketal methacrylate) P(FAMA-co-SoMA)

P(FAMA-co-SoMA) was prepared following the same polymerization procedure for PFAMA, with FAMA and SoMA as the monomers (1:1 mol ratio) in toluene. The dried polymer was then weighed, giving a mass of 0.6726 g. ^{1}H NMR (400 MHz, $CDCl_3$): δ 0.86 – 1.82 (b, 16 H, $H_{h\text{-}m}$), 3.73 – 4.33 (b, 5 H, H_e, Hf, H_g), 4.85 – 4.92 (b, 2 H, H_d), 6.33 – 6.37 (b, 2 H, H_b, H_c), 7.41 (b, 1 H, H_a); FT-IR (ν_{max}/cm): 1719 (-C═O).

2.3.6. Synthesis of poly(furfuryl alcohol methacrylate-co-lactic acid methacrylate) P(FAMA-co-LAMA) and poly(solketal methacrylate-co-lactic acid methacrylate) P(SoMA-co-LAMA)

P(FAMA-co-LAMA) was prepared using the same procedure for P (FAMA-co-SoMA) using ethyl acetate as the solvent. P(FAMA-co-LAMA) gave a mass of 0.85 g. ^{1}H NMR (400 MHz, $CDCl_3$): δ 0.18 – 2.00 (b, 10 H, H_e, H_f, H_i, H_j), 3.34 – 4.06 (b, 4 H, H_g, H_h), 4.94 (b, 2 H, H_d), 6.46 – 6.49 (b, 2 H, H_b, H_c), 7.66 (b, 1 H, H_a); FT-IR (ν_{max}/cm): 1719 (-C═O), 2500 – 3500 cm^{-1} (-COOH).

Similar reaction procedure was used in the synthesis of P(SoMA-co-LAMA). SoMA (0.60 g, 3.20 mmol), LAMA (0.50 g, 3.20 mmol) and ABCN (0.21 g, 0.84 mmol). ^{1}H NMR (400 MHz, $CDCl_3$): δ 1.20 – 2.09 (b, 16 H, H_d, H_e, H_f, H_g, H_j, H_k), 3.33 – 4.95 (b, 8 H, H_a, H_b, H_c, H_h, H_i); FT-IR (ν_{max}/cm): 1719 (-C═O), 2500 – 3500 cm^{-1} (-COOH),

2.3.7. Synthesis of film membranes

For a total mass of 500 mg, membranes based on cellulose triacetate (CTA) were fashioned by dissolving 300 mg of the CTA and 200 mg of the equivalent binding material (e.g. PSoMA/PFAMA) in 30 mL of chloroform. The solution was stirred using a magnetic stirrer until all membrane components had dissolved and poured into a petri dish, set horizontally and covered loosely. The resulting film was then cautiously peeled off the bottom of the petri dish after allowing the chloroform to evaporate for 24 h at room temperature. Likewise, the polysulfone (PSf)-based membranes were prepared.

2.3.8. Sol content and degree of swelling measurements

The swelling percentage of the membranes was calculated by placing a known dimension (1 cm × 1 cm) and weight (W_1) of film membrane samples in 20 mL of ethyl acetate. Ethyl acetate was selected to swell the polymeric membranes rather than dissolving the polymers at room temperature. After 24 h of swelling, the samples were then taken out, wiped with filter papers and weighed (W_2). The samples were dried again for 24 h to constant weight, and their weights were recorded as (W_3). The swelling percentage and sol content were calculated using the following formulae [30].

$$\text{Percentage of swelling} = \frac{W2 - w3}{W3} \times 100$$

$$\text{Sol content in percentage} = \frac{W1 - W3}{W1} \times 100$$

2.3.9. Hydrolytic degradation of film membranes

The polymeric membranes were cut into small pieces of dimensions $0.5cm \times 0.5cm$, and their initial weights were recorded as W_1. These cut pieces of polymeric membranes were transferred into five separate 50 mL beakers containing 10 mL of distilled water, 10 mL of 2% NaOH, 5% NaOH, 2% HCl and 5% HCl solutions, respectively. The samples were then taken out at designated times, wiped with filter paper and dried to constant weight. The weight was recorded as W_2, and the percentage weight loss was determined using the formula:[30].

$$\text{Percentage of weight loss} = \frac{W1 - W2}{W1} \times 100$$

3. Results and discussion

3.1. Reduction of furfural to furfuryl alcohol (FA)

Furfuryl alcohol (FA) was synthesized following a literature procedure reported in our group (Scheme S1) [26], as this led to 100% conversion and selectivity > 99%, which represents better performance (See Table S1) to those reported previously [31–36]. The successful reduction of the carbonyl group in furfural (FF) is confirmed from the ^{1}H NMR spectrum (Fig. S1 (a)). The appearance of a hydroxyl proton (H_e) at 2.51 ppm and methylene protons (H_d) at 4.55 ppm were observed.

Signals for all other protons are accounted for in their respective regions.

Also, its $^{13}C\{^1H\}$ NMR spectrum (Fig. S2) showed the disappearance of the carbonyl peak around 179 ppm and the appearance of a new signal at 57.35 ppm assigned to the methylene carbon, $\underline{C}H_2(OH)$. Infrared spectroscopy also revealed the disappearance of the carbonyl stretching frequency ν(C═O) around 1717 cm^{-1} (Fig. S3) with a broad OH peak at 3334 cm^{-1} thus, confirming the successful synthesis of furfuryl alcohol.

Solketal was prepared via an acetalization reaction, as has been reported in the literature [27]. The reaction was carried out under reflux at 60 °C to afford a colourless liquid in 51% yield. All spectroscopic evidence gathered support the successful formation of this compound.

3.2. Synthesis and characterization of methacrylated furfuryl, solketal and lactic acid monomers

Furfuryl alcohol methacrylate (FAMA) and Solketal methacrylate (SoMA) monomers were synthesized by a transesterification reaction following literature procedures [28,29]. (Scheme S2). The presence of two vinylic protons at 5.55 ppm and 6.11 ppm (H_{e1} and H_{e2}) confirm successful installation of the methacrylic group (Fig. S1(b)), and this is further supported by a downfield shift of H_d protons from 4.55 ppm (in FA) to 5.11 ppm (in FAMA) along with new methyl signal (H_f), at 1.92 ppm.

The identical vinylic and methyl protons appeared in the ^1H NMR spectrum of SoMA (Fig. S4(a)), thereby confirming the successful incorporation of the methacrylic group into solketal. Signals for all other protons were accounted for in their respective regions. $^{13}C\{^1H\}$ NMR spectra for both FAMA and SoMA exhibited carbon peaks assigned to the carbonyl, -C═O, and vinylic carbons $H_2\underline{C}═\underline{C}(CH_3)$ (Fig. S5 and S6, respectively). The disappearance of the broad -OH peak at 3334 cm^{-1} and the appearance of -C═O peak at 1717 cm^{-1} and -C═C peak at 1636 cm^{-1} in the infrared spectrum of FAMA also corroborated its synthesis (Fig. S3). Also, the disappearance of broad -OH peak at 3441 cm^{-1} and the presence of -C═O peak at 1719 cm^{-1} and -C═C peak at 1638 cm^{-1} in the IR spectrum of SoMA affirmed the successful synthesis of SoMA monomer (Fig. S7).

Lactic acid methacrylate monomer (LAMA) was synthesized by a slightly different protocol [25], where esterification between lactic acid and methacrylic acid was conducted in the presence of methane sulfonic acid (as a catalyst) and hydroquinone to prevent polymerization of methacrylic acid. (Scheme S3). Here too, the appearance of two vinylic proton signals at 5.62–6.20 ppm (H_a) and methyl resonance (H_c) at 1.92 ppm proved the proposed structure of the product being LAMA (Fig. S8(a)). $^{13}C\{^1H\}$ NMR spectrum showed carbon peaks assigned to the carbonyl, -C═O, and vinylic carbons $H_2\underline{C}═\underline{C}(CH_3)$ (Fig. S9). Also, the appearance of a very broad -COOH peak around 2500–3500 cm^{-1}, -C═O peak at 1705 cm^{-1}, and -C═C peak at 1628 cm^{-1} in the IR spectrum of LAMA corroborated the successful synthesis of LAMA monomer. (Fig. S10).

3.3. Homo-polymerization of FAMA, SoMA and LAMA

Free radical homo-polymerization of FAMA and SoMA via solution polymerization was performed with 1,1-Azobis(cyclohexanecarbonitrile) (ABCN) as the initiator in toluene (Scheme S4 (a), (b)). FAMA and SoMA polymers were found to be soluble in toluene at the polymerization temperature and room temperature. There were no ring-opening products following homo-polymerization of FAMA and SoMA.

Compared to the ^1H NMR spectrum of FAMA (Fig. S1(b)), the ^1H NMR of PFAMA (Fig. S1(c)) exhibited disappearance of vinylic protons (5.55–6.11 ppm) together with the appearance of methylene backbone protons (H_e) at 0.85–1.22 ppm, thereby confirming the formation of the polymer. Also, the presence and broadening of other peaks (H_a, H_b, H_c, H_d) corroborated the retention of the ring structure.

Similarly, the disappearance of vinylic protons (at 5.55–6.11 ppm) and the appearance of methylene backbone protons (H_a) at 1.83–2.12 ppm in the ^1H NMR spectrum of PSoMA (Fig. S4(b)) confirmed its formation. Again, the presence and broadening of other peaks (H_c, H_d, H_e) affirmed the retention of the ring. Moreover, the infrared spectrum of PFAMA (Fig. S3) and PSoMA (Fig. S7) exhibited disappearance of -C═C peak at 1636 cm^{-1} and 1638 cm^{-1}, respectively hence supporting the successful polymerization of FAMA and SoMA.

A similar polymerization technique was used to homo-polymerize lactic acid methacrylate monomer (LAMA), with ethyl acetate being used as the solvent. (Scheme S4 (c)) The highly polar nature of the polymer led to precipitation during the polymerization in ethyl acetate (termed precipitation polymerization). Hence the polymer was found to be insoluble in ethyl acetate at both polymerization temperature and room temperature. Like PLAMA, the successful homo-polymerization of LAMA was confirmed by the ^1H NMR spectrum and FTIR results (Fig. S8 (b) and S10). Homo-polymerization results are provided in Table S2.

3.4. Synthesis of poly(FAMA-co-SoMA)

Free radical co-polymerization of FAMA with SoMA (in a feed ratio of 1:1/50:50) via solution polymerization technique was performed using 1,1-Azobis(cyclohexanecarbonitrile) (ABCN) as the initiator and toluene as solvent (Scheme 1). The reactions were carried out under reflux at 88 °C with continuous stirring for 24 h. The co-polymer was found to be soluble in toluene at the polymerization temperature and room temperature.

The co-polymer composition ratios between FAMA and SoMA in the polymer was calculated (based on equation [25] (1)) to be 58:42, respectively.

$$X_{FAMA} = \frac{(N_{SoMA})(I_{HFAMA})}{(N_{SoMA})(I_{HFAMA}) + (N_{FAMA})(I_{HSoMA})} \quad (1)$$

where X_{FAMA} corresponds to the molar fraction of FAMA in the co-polymer, I_{HFAMA} is the integral value concerning the peak marked with the letter (d) (related to FAMA monomer) in the molecular structure of P (FAMA-co-SoMA); I_{HSoMA} is the integral value concerning the peak marked with the letter (g) (related to SoMA monomer) in the molecular structure of P(FAMA-co-SoMA); N_{FAMA} is the number of protons related to the peak (d) and N_{SoMA} is the number of protons related to the peak (g).

This showed that FAMA and SoMA could co-polymerize well though FAMA tends to be more reactive than SoMA. The ability of FAMA and SoMA to co-polymerized well is due to the similarities in their polarities. Relative to the ^1H NMR spectra of FAMA and SoMA, the ^1H NMR spectrum of P(FAMA-co-SoMA) exhibited the disappearance of vinylic protons (5.55–6.11 ppm) (Fig. 1). The appearance of methylene backbone protons (H_e) peaks at 0.85 – 1.22 ppm also supported the polymer formation. Again, the presence of other peaks (H_a, H_b, H_c, H_d) validated the retention of the ring structure. The disappearance of -C═C peak at 1637 cm^{-1} in the FTIR spectrum of P(FAMA-co-PSoMA) (Fig. S11) also supported the successful co-polymerization of FAMA and SoMA.

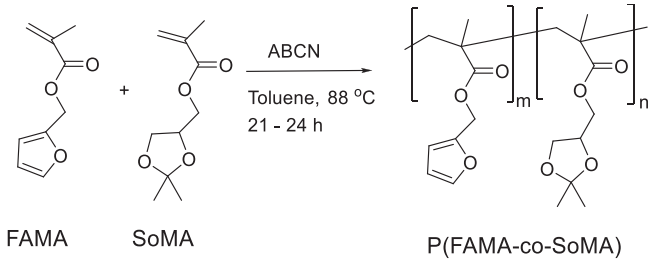

Scheme 1. Outline of the co-polymerization of FAMA and SoMA.

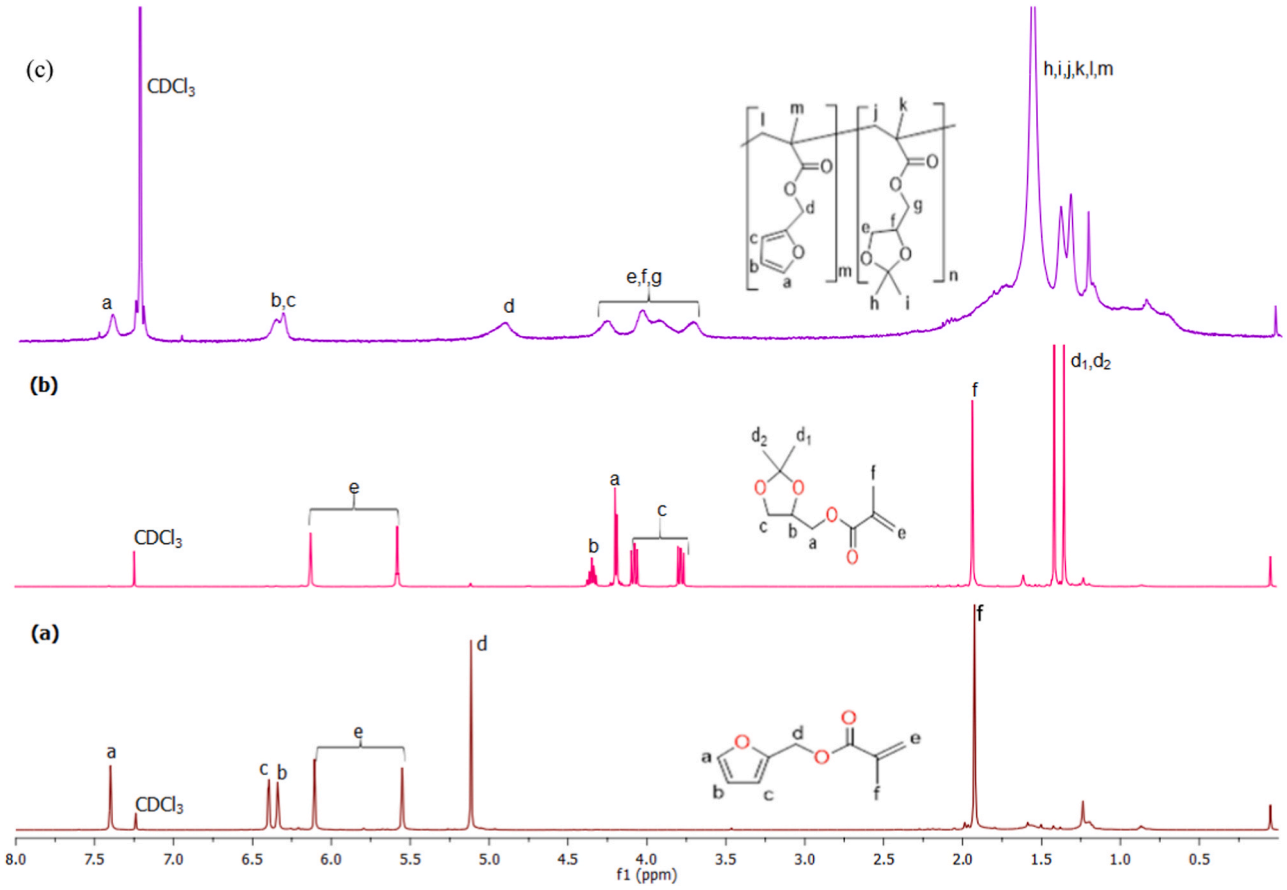

Fig. 1. ^{1}H NMR spectra of (a) FAMA; (b) SoMA and (c) P(FAMA-co-SoMA).

3.5. Synthesis of Poly(FAMA-co-LAMA) and Poly(SoMA-co-LAMA)

Free radical co-polymerization of FAMA and LAMA (in a feed ratio of 1:1/50:50) via solution polymerization technique was performed using 1,1-azobis(cyclohexanecarbonitrile) (ABCN) as an initiator and ethyl acetate as solvent (Scheme 2a). Ethyl acetate was chosen as the solvent to ensure effective polymerization since both monomers (FAMA and LAMA) were found to be miscible in it. The reactions were carried out under reflux at 80 °C with continuous stirring for 24 h. P(FAMA-co-LAMA) was soluble in ethyl acetate at the polymerization temperature but insoluble at room temperature. The co-polymer composition ratio between FAMA and LAMA in the polymer was calculated to be 70:30, respectively. Thus, FAMA tends to be more reactive than LAMA, which might be ascribed to the aromatic nature of the furan ring.

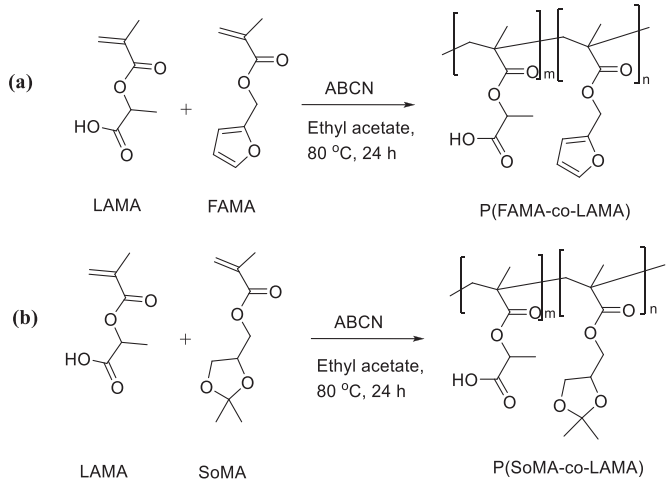

Scheme 2. Outline of the co-polymerization of **(a)** FAMA and LAMA and **(b)** SoMA and LAMA.

Similar feed ratio, polymerization technique, solvent, polymerization temperature and time were employed in the free radical co-polymerization of SoMA and LAMA (Scheme 2b).

However, P(SoMA-co-LAMA) was found to be insoluble in ethyl acetate at both polymerization temperature and room temperature. This insolubility can be ascribed to the polar nature of interactions due to the lactic acid group. The co-polymer composition ratio between SoMA and LAMA in the polymer was calculated to be 44:56, respectively. This shows that SoMA and LAMA could co-polymerize well though LAMA tends to be more reactive than SoMA due to the similarities in their polarities. However, the higher reactivity of LAMA might be attributed to the carboxylic acid functional group, whereas steric hindrance in SoMA might be a reason for its lower percentage composition.

The successful free radical co-polymerization of FAMA with LAMA and SoMA with LAMA was confirmed by ^{1}H NMR spectroscopy. ^{1}H NMR spectrum of P(FAMA-co-LAMA) (Fig. 2 (c)) exhibited the disappearance of vinylic protons (5.55–6.23 ppm), which were present in the ^{1}H NMR spectra of FAMA (Fig. 2 (b)) and LAMA (Fig. 2 (a)). The appearance of methylene backbone protons (H_e, H_i) peaks in the range of 0.85 – 1.88 ppm also supported the polymer formation. Also, the presence of (H_a, H_b, H_c, H_d) peaks and other peaks corroborated the retention of the ring structure in FAMA.

^{1}H NMR spectrum of P(SoMA-co-LAMA) depicted the identical disappearance of vinylic protons (5.55–6.23 ppm) (Fig. 3(c)) together with the appearance of methylene backbone protons (H_e, H_f, H_j) peaks in the range of 0.85 – 1.88 ppm hence successful formation of the polymer. The disappearance of -C═C peak at 1628 cm^{-1} (in LAMA) and 1636 cm^{-1}

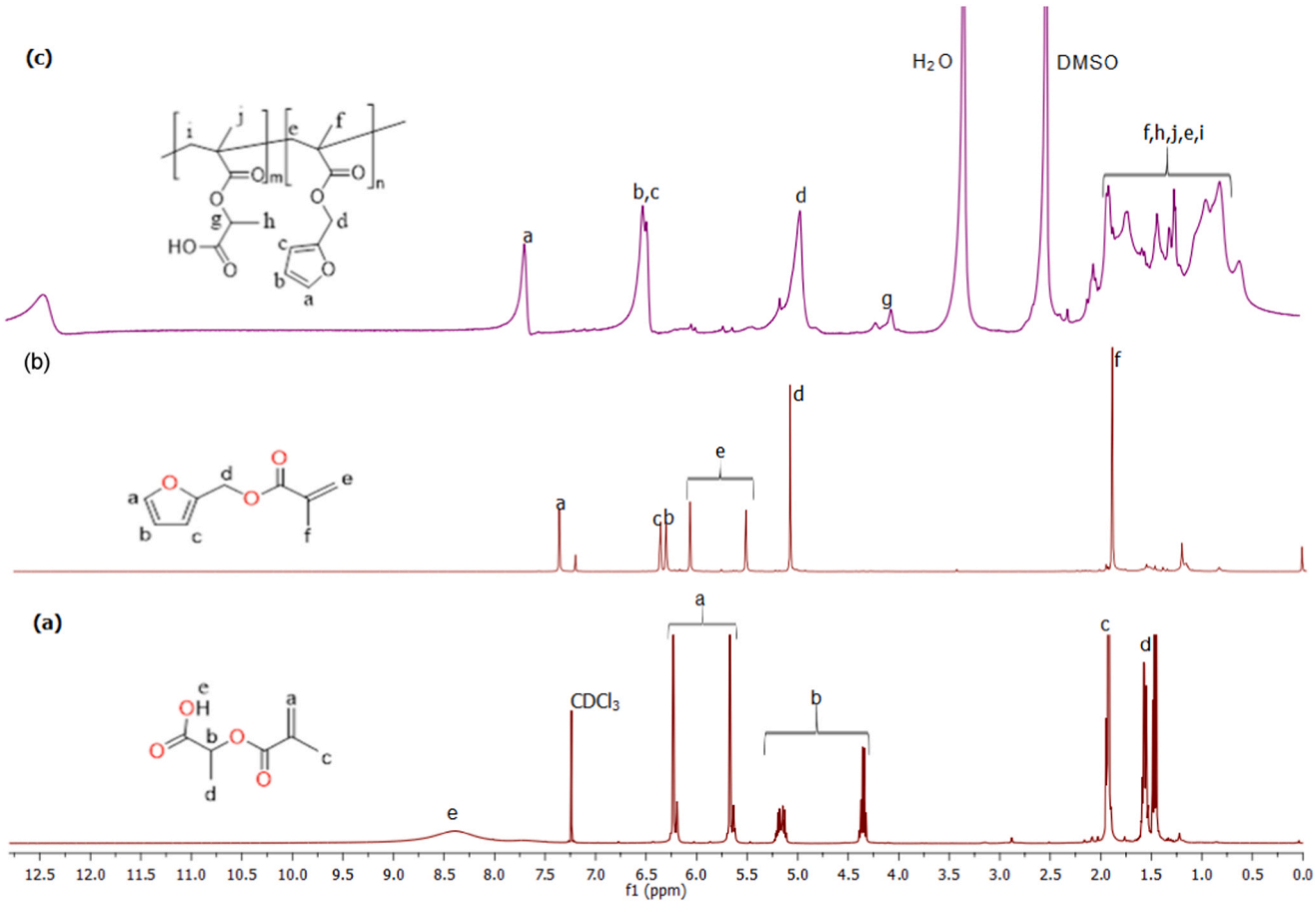

Fig. 2. ^{1}H NMR spectra of (a) LAMA; (b) FAMA and (c) P(FAMA-co-LAMA).

(in FAMA) in the FTIR spectrum of P(FAMA-co-LAMA) (Fig. S12) also supported the successful co-polymerization of FAMA and LAMA. Similarly, there was the disappearance of -C═C peak at 1628 cm^{-1} (in LAMA) and 1638 cm^{-1} (in SoMA) in the FTIR spectrum of P(SoMA-co-LAMA) (Fig. S13) hence successful co-polymerization of SoMA and LAMA. Copolymerization results are provided in Table S3.

3.6. Molecular weight, thermal properties and powder X-ray diffraction analyses

3.6.1. Molecular weight

The molecular weight of the polymers was ascertained using size exclusion chromatography (SEC) (Table 1.0). Also, the chromatograms of all the polymers are shown in Fig. S14, Fig. S15 and Fig. S16. The number average molecular weight (M_n) and weight average molecular weight (M_w) range in 7500–2200 $gmol^{-1}$ and 29400–2600 $gmol^{-1}$, respectively. The insolubility of P(SoMA-co-LAMA) in a wide range of solvents made it quite challenging to measure the true molecular weight using the room temperature SEC technique, hence the lowest molecular weight value of 2200 $gmol^{-1}$. The dispersity index (Đ) ranges from 4.1 to 1.2. Thus, all the polymers have a broad molecular weight distribution with different chain lengths. It can also be inferred that the polymers were fashioned randomly and could display their effect on numerous characteristics of polymeric materials.

3.6.2. Differential scanning calorimetry analysis (DSC)

DSC thermograms of both homopolymers and co-polymers are shown in Fig. S17. The glass transition temperature (T_g) values were obtained from the first midpoint of transition on the curves. Crystalline temperature (T_c) and melting point temperature (T_m) were also identified on the curves that confirm crystalline regions in the polymers. Complete amorphous polymers would not show T_c and T_m. The T_g values of the polymers spread over a range of 150 °C and 67 °C. (Table 1), which are comparable to the T_g of some commercially available polymers (such as poly(ethylene terephthalate) (PET, T_g = 76 °C), poly (ethylene 2,5-furanoate) (PEF, T_g = 81 °C) and poly(methyl-methacrylate) (PMMA, T_g = 105 °C).

T_g depends on the flexibility and mobility of the polymeric chains, which generally depend on several factors like chain stiffness of the polymer, intermolecular forces, bulky and flexible pendant groups, molecular weight, cross-linking etc [37]. Stiffening groups (such as carbonyl, sulfone, amide, aromatic etc.) present in polymer chains decrease the chain's flexibility, hence increasing the T_g [37].

The T_g values of the polymers increased as follows: PSoMA < PFAMA < P(FAMA-co-SoMA) < PLAMA < P(SoMA-co-LAMA) < P(FAMA-co-LAMA). Notably, the furan ring tends to restrict the flexibility of the polymer chain in PFAMA, thus leading to a slight increase in the T_g value of PFAMA.

Moreover, T_g of the polymers containing the LAMA moiety [P(SoMA-co-LAMA), P(FAMA-co-LAMA)] was noticed to be higher than those without the LAMA. This can be ascribed to the carboxylic acid functional group (-COOH) in LAMA, contributing to much stronger hydrogen bonding between the hydroxyl and carbonyl groups. Comparing the T_g of P(FAMA-co-LAMA) and P(SoMA-co-LAMA), the former had a higher T_g of 150 °C due to the stiffening group (furan ring) in the FAMA.

The order of the melting point of the polymers were as follows; PSoMA (195–200 °C) < PFAMA (205–210 °C) < PLAMA (220–225 °C) < P(FAMA-co-LAMA) (245–250 °C) < P(FAMA-co-SoMA) = P(SoMA-co-LAMA) (270–275 °C). Therefore, the co-polymers have a higher degree of crystallinity than the homopolymers due to their higher melting

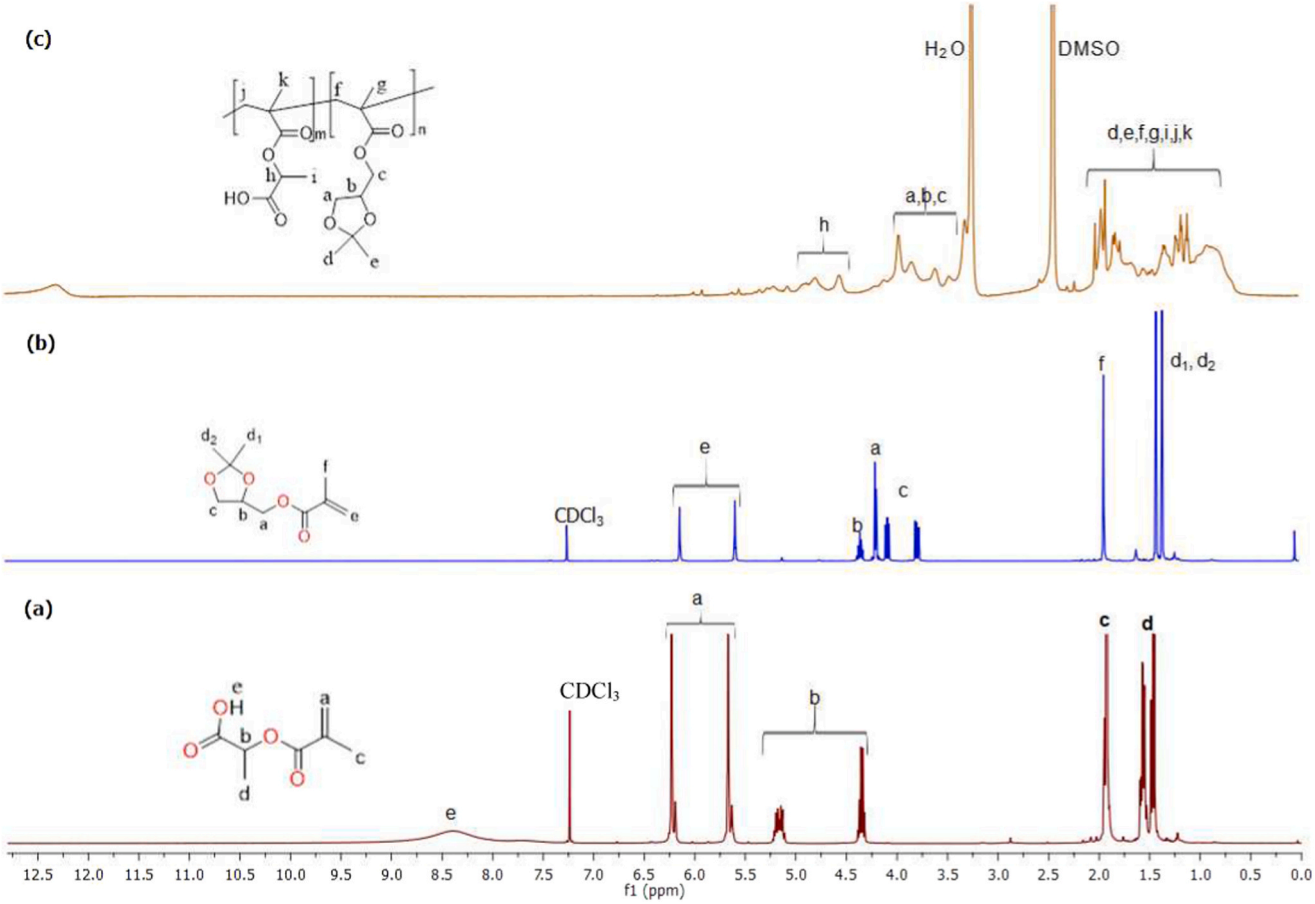

Fig. 3. ^{1}H NMR spectra of (a) LAMA; (b) SoMA and (c) P(SoMA-co-LAMA).

Table 1
Molecular weight (M_n, M_w), dispersity index (Đ), glass transition temperature (T_g) and degradation temperature of homo and co-polymer samples.

Sample	M_n (g/mol)	M_w (g/mol))	Đ (M_w/M_n)	T_g (°C)	T_d (°C)
PFAMA	3700	8700	2.4	70	155
PSoMA	7500	18,400	2.5	67	155
P(FAMA-co-SoMA)	5200	18,800	3.6	74	150
P(FAMA-co-LAMA)	5400	14,800	2.7	150	155
P(SoMA-co-LAMA)	2200	2600	1.2	100	155

point. Also, co-polymers containing the SoMA moiety had higher T_m than those without the SoMA. This can be attributed to the strong intermolecular interaction in the polymer chains.

3.6.3. Thermogravimetric (TGA) and powder X-ray diffraction analyses

Thermogravimetric curves of the polymers are shown in Fig. S18. The temperatures used for the study were between 25 °C and 600 °C. PSoMA, PFAMA, P(SoMA-co-LAMA) and P(FAMA-co-LAMA) showed thermal stability up to ~ 155 °C whilst P(FAMA-co-SoMA) and PLAMA showed thermal stability up to ~ 150 °C and ~ 125 °C, respectively. A slight weight loss of about 5% was observed in P(FAMA-co-SoMA) and PSoMA, P(SoMA-co-LAMA), PFAMA, P(FAMA-co-LAMA) at 155 °C and 200 °C, respectively. This can be attributed to dehydration in the polymer materials. Moreover, 20% (by mass) of the materials degrade around 350 °C for P(SoMA -co-LAMA) and P(FAMA-co-LAMA), 325 °C for PSoMA, 300 °C for PFAMA and P(FAMA-co-SoMA), indicating good thermal stability. However, 20% of PLAMA material was found to degrade around 200 °C; thus, PLAMA showed the least thermal stability. All the polymers went through no less than three phases of disintegration, with the first stage being attributed to dehydration. In contrast, the last two stages are probably due to the disintegration of ester bonds, acetal bonds and furan rings. The residual weight at 600 °C decreased as follows: PFAMA > P(FAMA-co-SoMA) > P(FAMA-co-LAMA), PLAMA > PSoMA > P(SoMA-co-LAMA), suggesting that residual weight is associated with the rigid aromatic group in content for the furan-based methacrylic polymers.

The PXRD graph of both the homopolymers and co-polymers, shown in Fig. 4, revealed a broad characteristic peak around $2\theta = 20^{o}$ and some sharp but less intense peaks in the range of $2\theta = 25–60°$. This indicates that the polymers contain high amorphous regions and low or partial crystalline regions. Thus, they are semi-crystalline and would be prone to degradation either hydrolytically or photolytically. PFAMA has the highest degree of partial crystallinity while PSoMA has the lowest degree of partial crystallinity.

3.6.4. Transmission electron microscopy (TEM) analyses

TEM micrographs of the polymers are shown in Fig. 5. Notably, nanoparticles were identified in the micrograph of P(FAMA-co-SoMA), PFAMA and PSoMA, indicating nanostructured materials. Larger particles of an average diameter of 35 nm were measured in P(FAMA-co-SoMA) compared to smaller particle sizes in PFAMA and PSoMA. Darker regions in the micrograph of PSoMA indicate a denser packing of particles which correspond to fewer electrons reaching the fluorescent screen. However, the micrograph of P(FAMA-co-LAMA) and P(SoMA-co-LAMA) did not show any nanoparticles but rather a sheet.

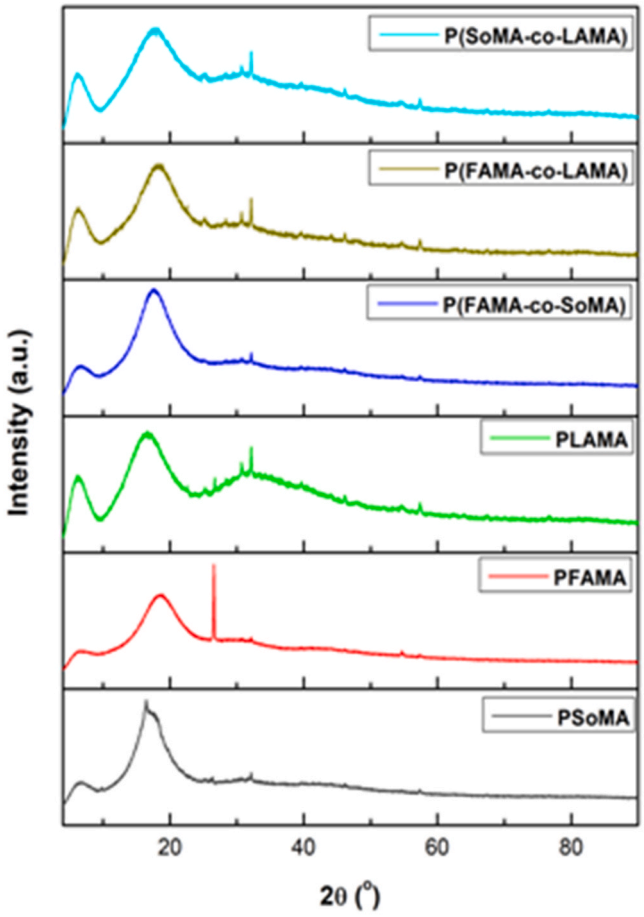

Fig. 4. XRD Patterns of synthesized polymers.

3.6.5. Scanning electron microscopy (SEM) analyses

SEM micrographs of the polymers shown in Fig. 6 reveals that all the polymers are non-fibrous and powdery in texture. Moreover, the lactic acid methacrylate-based polymers tend to form more clusters of particles than the furfural and solketal based polymers.

3.6.6. Membrane preparation

Attempts to form film membranes from the synthesized polymers (PFAMA, PSoMA and PFAMA-co-SoMA) by solvent casting method proved unsuccessful as the polymer membrane got stuck on the glass surface and had visible cracks. Hence, they were blended with commercially available polymers like polysulfone (Psf) and cellulose acetate (CTA), which lead to the formation of better membranes (Fig. 7).

Films were fabricated using a ratio of the mass of Psf to the synthesized polymer mixture (1.5:1). The exact ratio was employed in the CTA-based membranes. Seemingly robust films were created from the evaporation of the solvent over a minimum of 48 h period at room temperature.

Although chloroform served as a suitable casting solvent, numerous variables had to be optimized before obtaining a moderately combined polymer composite solvent-cast method. A mass ratio of 1:10 (chloroform to polymer composite) was found to be optimal. Utilizing solutions with much lower proportions of chloroform to polymer composite (e.g. 1:3) resulted in a much thinner film after solidification due to less polymer composite in the final substrate with similar volumes of the mixture. Increasing the ratio (e.g. 1:30) formed a solution much higher in viscosity, resulting in a material that was laborious to process and eventually a blend that would not settle into a homogenous thickness before attaining the critical evaporation point of the chloroform and solidification. Comparing membranes from Psf and CTA based with CTA based membranes, it was observed that CTA membranes would occasionally fracture or tear when attempts were made to remove them from the petri dish to make the membranes. The brittle nature of the CTA membranes could be due to thin membranes but could also be due to their inherent brittle nature. This effect was much more significant in the CTA-PSoMA membrane.

Another variable that needed cautious control was the chloroform evaporation rate. If the chloroform evaporation rate was too fast and in an uncontrolled manner, this led to the re-agglomeration of the polymer composite in the solution. As a result, the dish was covered very tightly during the initial solvent evaporation. This helped reduce the evaporation rate by changing the comparative partial pressure of the chloroform in the air space and thus the diffusion rate across the free surface boundary.

It should be noted that processing polymer composites via solvent -casting has some magnificent potential to make composite membranes of this nature more captivating. Although the final material thickness would be perfect for a thin film and coating, the constraints on the thickness and uniformity identified in this study may be raised with more improved techniques.

3.6.7. Microscopy analysis of film membranes

Transmission electron microscopy (TEM) micrographs of the film membranes are shown in Fig. S19 below. Remarkably, nanoparticles were identified in the micrograph of PSf-PFAMA and CTA-PFAMA-co-SoMA, indicative of a nanostructured material. Darker areas in the micrograph of CTA-PFAMA-SoMA indicate a denser packing of particles which correspond to fewer electrons reaching the fluorescent screen. However, the micrograph of PSf-PSoMA, PSf-PFAMA-co-SoMA, CTA-PFAMA, CTA-PSoMA did not show any nanoparticles but rather a sheet.

Scanning electron microscopy (SEM) micrographs of the membranes are shown in Fig. S20 below. Notably, pores with varying sizes were identified on the surfaces of all the membranes. Among the PSf based membranes, PSf-PFAMA exhibited a high surface porosity with tiny pores randomly distributed on the membrane surface. At the same time, PSf-PFAMA-SoMA showed a low surface porosity with small pores randomly distributed on the membrane surface. With the CTA based membranes, CTA-PFAMA portrayed a high surface porosity with large pores randomly distributed on the membrane surface relative to the low surface porosity observed in CTA-PSoMA and CTA-PFAMA-PSoMA membranes. PSf-PFAMA, PSf-PFAMA-SoMA, CTA-PFAMA, and CTA-PSoMA membranes had smooth surfaces, while PSf-PSoMA and CTA-PFAMA-SoMA membranes had rough surfaces. Therefore, it can be inferred that the furfural-based membranes tend to exhibit high surface porosity with a smooth surface compared to the solketal based membranes.

3.6.8. PXRD analysis of film membranes

The PXRD graph of both Psf and CTA based film membranes are shown in Fig. S21. The XRD patterns of the membranes exhibited a distinct broad characteristic peak around $2\theta = 20–40^{\circ}$ without any noticeable sharp peaks. This indicates the complete amorphous nature of the membranes relative to the semi-crystalline nature of the synthesized polymers. The amorphous nature of the membranes can be attributed to reinforcing the synthesized polymers with the commercial polymers (Psf and CTA). It would mean the membranes would be easily degraded at the end of use.

3.6.9. Swelling studies and Sol content

The swelling percentage of the polymeric membranes in ethyl acetate are set out in Table 2. Swelling of a polymer is defined as the penetration of a solvent into the polymer network resulting in a sharp change in the volume of the polymer [38]. Swelling behaviour depends on the solvent, hydrophilic/hydrophobic nature of the polymer and cross-linking density. A highly cross-linked polymer conveys a minor degree of swelling [30]. All the polymer composite membranes showed

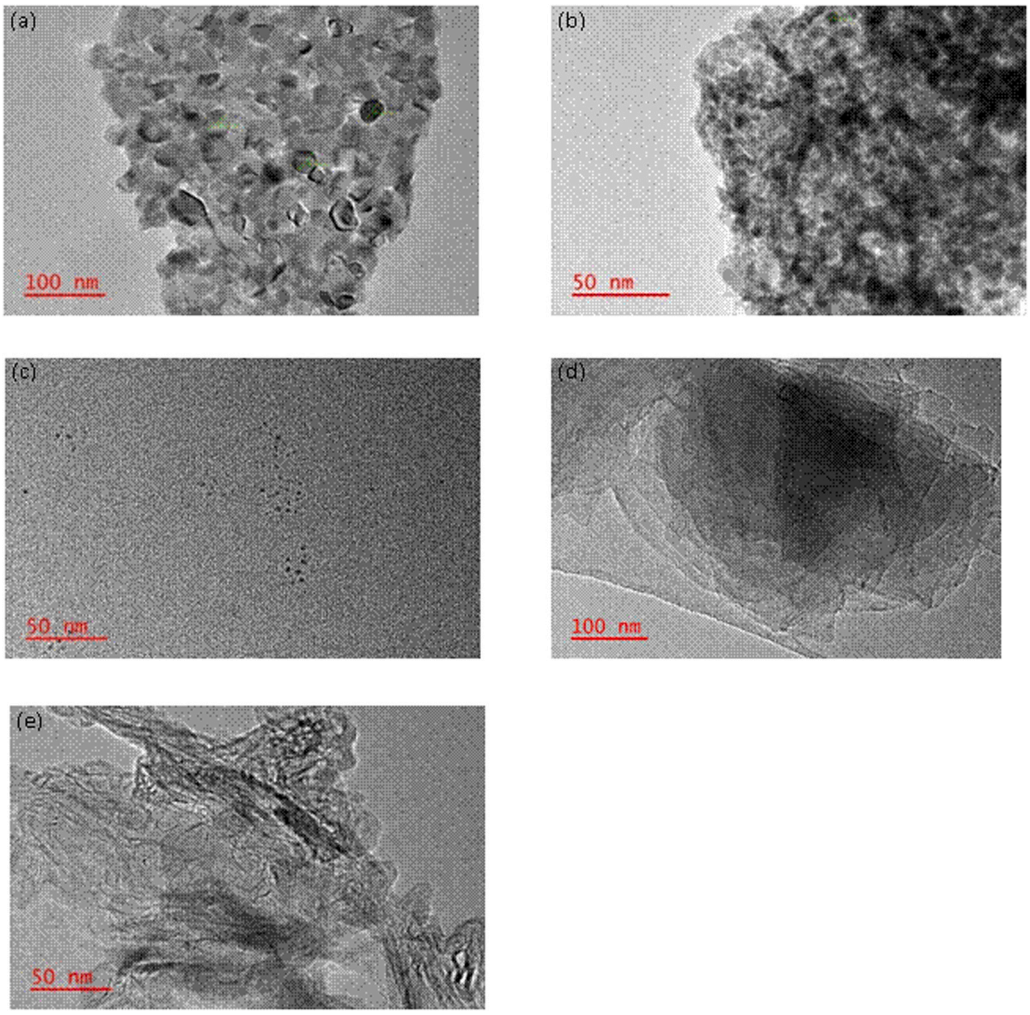

Fig. 5. TEM micrograph of: (a) P(FAMA-coSoMA), (b) PSoMA, (c) PFAMA, (d) P(SoMA-co-LAMA) and (e) P(FAMA-co-LAMA).

a high swelling percentage, with the least value being 64.12%. Fig. S22 shows the image of the polymer membrane before and during swelling. This is indicative of low cross-linking in the polymer composite membrane. The variation in the percentage of swelling values might be attributed to the differences in their hydrophilicity.

The sol content percentage of the polymer membranes are recorded in Table 2. There are some fractions of free polymer in cross-linked polymers that may not be attached to the polymer network. This fraction of free polymer is known as the sol fraction or sol content of the polymer. This sol fraction diffuses out of the membrane to the solvent bath during swelling [30]. In exploring the application of polymers in the biomedical field, the study of diffusion of loose sol fractions in the swollen state plays a significant role. Hence, these polymer membranes may find application in the biomedical field.

3.6.10. Hydrolytic degradation studies

Hydrolytic degradation studies of the polymeric membranes were done in alkaline and acidic solutions of different concentrations at room temperature. Fig. 8 illustrates the change in weight of polymeric membranes in alkaline and acidic solutions at different times. Notably, there was a minimum weight loss of 10% regardless of the concentration and time in all the membranes. Also, the weight loss of the polymeric membranes increased slightly with an increase in the concentration of NaOH/HCl and time. Among the polysulfone (PSf) based membranes, PSf-PSoMA recorded the highest weight loss in HCl solution at different concentrations and time. This might be due to the presence of acetyl groups in PSoMA, which are known to undergo hydrolysis in acidic solution (i.e. deacetylation), thereby enhancing the degradation rate.

Moreover, comparing the PSf and CTA based membranes, CTA based membranes recorded higher weight loss in both NaOH and HCl solutions. Deacetylation of the acetyl groups in CTA and hydrolysis of glycosidic bonds in cellulose chains accounted for such weight loss. Though there was no complete weight loss of the membranes in 72 h, it is clear from the degradation studies that complete hydrolytic degradation could be possible over two to three months since weight loss was observed to increase with time.

3.6.11. Degradation studies in seawater

The degradation of polymeric membranes in seawater was studied for twenty days at room temperature. Fig. S23 illustrates the change of weight of polymeric membranes in seawater. All the membranes exhibited some degree of degradation, with PSf-PFAMA recording the lowest percentage weight loss of 4%.

Comparing the PSf and CTA based membranes, CTA based membranes recorded higher weight loss. This might be due to the deacetylation of the acetyl groups in CTA against the stable sulfone groups in PSf.

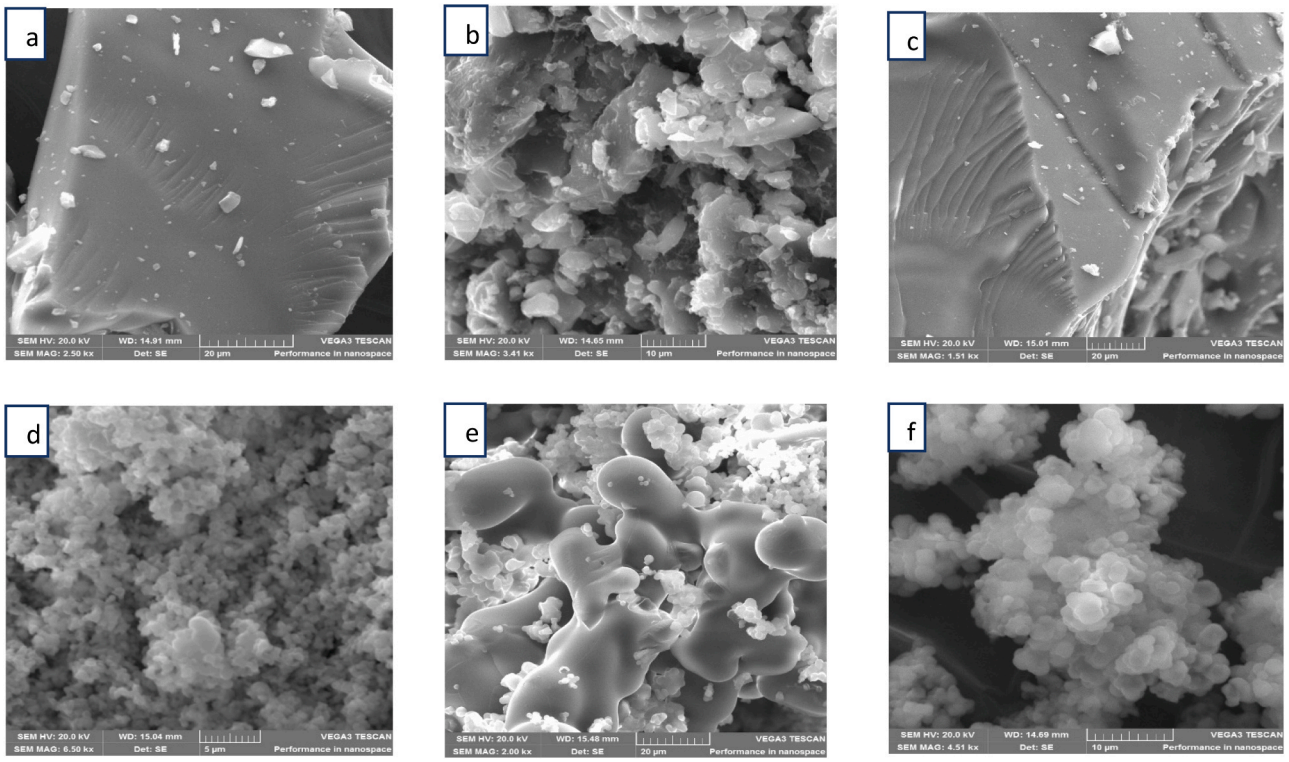

Fig. 6. SEM micrograph of: (a) PFAMA; (b) PSoMA; (c) P(FAMA-co-SoMA); (d) P(FAMA-co-LAMA); (e) P(SoMA-co-LAMA); (f) PLAMA.

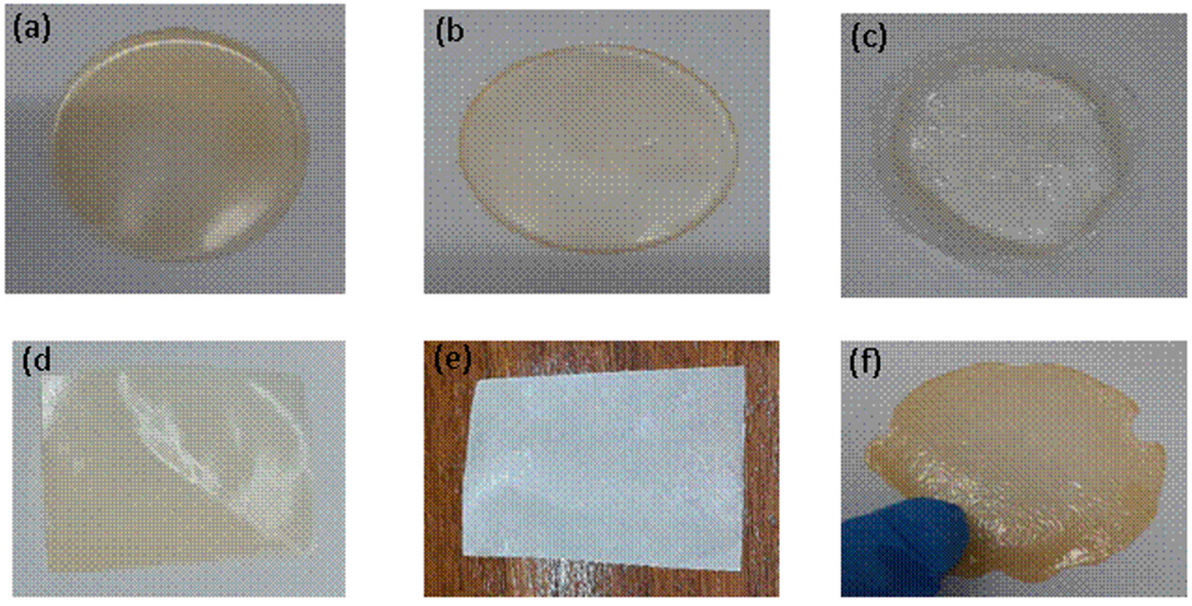

Fig. 7. Images of film membranes: (a) CTA-P(FAMA-co-SoMA); (b) CTA-PFAMA; (c) CTA-PSoMA; (d) PSf-PFAMA; (e) PSf-PSoMA; (f) PSf-P(FAMA-co-SoMA).

Table 2
Swelling and sol content percentage of Polymer membranes.

Polymer	Swelling % in Ethy1 acetate	Sol content in percentage
Psf-PFAMA	79.49	20.95
Psf-PSoMA	81.67	26.65
Psf-P(FAMA-co-SoMA)	64.12	23.01
CTA-P(FAMA-co-SoMA)	81.11	17.90
CTA-PFAMA	80.50	17.00

4. Potential application of polymeric membranes

4.1. Coating application

Pieces of metal and wood surfaces were coated with CTA/PFAMA-SoMA and PSf/PSoMA membranes, respectively. The images of the surfaces before and after coating are shown in Fig. S24. The coating obtained from the metal surface was translucent and less glossy, while the wood surface gave a transparent and glossy look. The membranes could prove useful in waterproof coating surfaces.

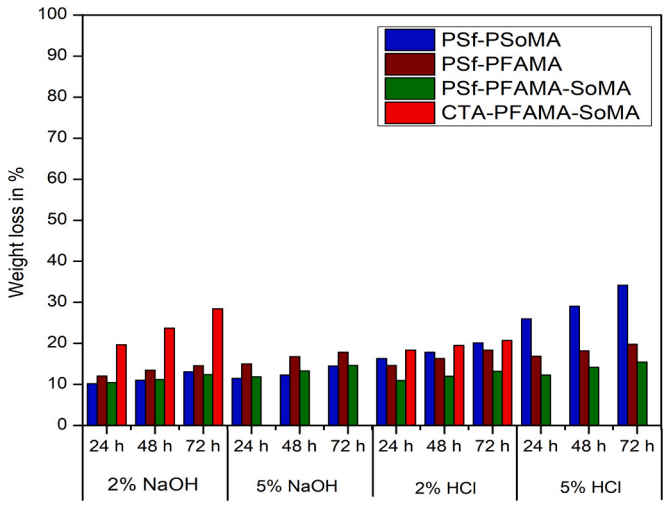

Fig. 8. Hydrolytic degradation of film membranes in basic and acidic solutions.

4.2. Water filtration application

To study the ability of water to permeate through the membranes, deionized water in a dead-end cell was employed. Compressed nitrogen gas was used to regulate the water flow pressure. The membranes were pressurized at 1200 KPa for 20 min to compact them before assessment. At distinct pressures (400, 600, 800 and 1000) kPa, pure water flux (J_{flux}) was noted within 10 min intervals. The permeation flux was calculated using the equation below:

$$J_{flux} = \frac{V}{A \times t}$$

Where J_{flux} is the permeation flux of the membrane for pure water (Lm $^{-2}$ h^{-1}), 'v' is the volume of permeate water (L), 'A' is the effective area of the membrane (m^2) and 't' is the permeation time (h). The water flux increased with an increase in flow pressure (Table 3 and Fig. S25). Thus, more water permeates through the PSf-PFAMA membrane as the pressure was increased. This means that the Psf-PFAMA membrane can be applied in water filtration. However, water permeation through the other PSf-based membranes (i.e. Psf-PFAMA-co-SoMA and PSf-PSoMA) was unsuccessful. Moreover, the CTA based membranes could not stand the pressure in the dead-end cell due to their thin and brittle nature. As a result, they broke off quickly, making them unsuccessful for the water flux test.

5. Conclusion

Furfuryl alcohol, Solketal and lactic acid methacrylate monomers were synthesized successfully from bio-based chemicals furfural, glycerol and lactic acid. The monomers were synthesized with high yield and purity using scalable, simple reaction conditions and post-work up procedures. Free radical homo and co-polymerization of the monomers were successful. The ^{1}H NMR and FTIR spectrum confirmed the chemical structure of the polymers. Moreover, the polymers exhibited good thermal stabilities (in the range of 125–155 °C) and glass transition temperature (T_g) over a range of 150–67 °C. Notably, the polymers were semi-crystalline and had T_g comparable to those of some commercially available polymers (such as; poly ethylene terephthalate (PET), poly (ethylene 2,5-furanoate) (PEF) and poly(methylmethacrylate) (PMMA), which have T_g of 76 °C, 81 °C and 105 °C respectively. Also, the PXRD graph and the melting point and crystalline temperature identified in the DSC thermogram support the semi-crystalline nature of the polymers.

Furthermore, furfuryl alcohol and solketal methacrylate polymers (PFAMA, PSoMA and P(FAMA-co-SoMA)) were reinforced successfully using commercially available cellulose triacetate (CTA) and polysulfone (PSf) to give new amorphous polymer composites which have promising degradation attributes, as they demonstrated hydrolytic degradation of 10% in 24 h. When fashioned into membranes, the polymer composites were found to have potential coatings and water filtration applications.

Table 3
Water flux test on Psf/PFAMA membrane at time intervals of ten minutes.

Pressure (kPa)	Volume (L)	Flux ($Lm^{-2}h^{-1}$)
400	0.0022	102.71
600	0.0024	112.04
800	0.0026	121.38
1000	0.0028	130.72

CRediT authorship contribution statement

Raynold Techie-Menson: Conceptualization, methodology, Data collection & original draft. **Charles K. Rono:** Methodology (synthesis) & data analysis. **Anita Etale:** Analysis of the composites. **Gift Mehlana:** Thermal analysis of the polymers. **James Darkwa:** Conceptualization and Supervision. **Banothile C.E. Makhubela:** Conceptualization, Supervision, Funding acquisition. All authors participated equally in the manuscript review, editing & revisions.

Declaration of Competing Interest

The authors declare that they have no known competing financial interests or personal relationships that could have appeared to influence the work reported in this paper.

Acknowledgement

This work was supported by the Royal Society and African Academy of Sciences Future Leaders-African Independent Researchers (FLAIR) Scheme funded by the UK Government's Grand Challenges Research Fund (GCRF) (Fellowship ref: FLR_R1_191779), the National Research Foundation of South Africa (NRF) under grant numbers: 105558 and 117989 and the University of Johannesburg Research Centre for Synthesis and Catalysis. The use of UJ analytical facilities at SPECTRUM is acknowledged. The authors also thank Prof. Moutloadi for allowing us to use his dead-end cell filtration instrument.

Appendix A. Supporting information

Supplementary data associated with this article can be found in the online version at doi:10.1016/j.mtcomm.2021.102721.

References

[1] M.F. Sainz, J.A. Souto, D. Regentova, M.K.G. Johansson, S.T. Timhagen, D. J. Irvine, P. Buijsen, C.E. Koning, R.A. Stockman, S.M. Howdle, A facile and green route to terpene derived acrylate and methacrylate monomers and simple free radical polymerisation to yield new renewable polymers and coatings, Polym. Chem. 7 (2016) 2882–2887.
[2] M. Okada, Changes in ontogenetic expression of estrogen receptor alpha and not of estrogen receptor beta in the female rat reproductive tract, J. Mol. Endocrinol. 28 (2002) 87–97.
[3] J. Hopewell, R. Dvorak, E. Kosior, Plastics recycling: challenges and opportunities, Philos. Trans. R. Soc. Lond. B Biol. Sci. 364 (2009) 2115–2126.
[4] S.A. Miller, Sustainable polymers: replacing polymers derived from fossil fuels, Polym. Chem. 5 (2014) 3117–3118.
[5] P. Anastas, N. Eghbali, Green chemistry: principles and practice, Chem. Soc. Rev. 39 (2010) 301–312.
[6] Y. Zhu, C. Romain, C.K. Williams, Sustainable polymers from renewable resources, Nature 540 (2016) 354–362.
[7] C. Vilela, A.F. Sousa, A.C. Fonseca, A.C. Serra, J.F.J. Coelho, C.S.R. Freire, A.J. D. Silvestre, The quest for sustainable polyesters – insights into the future, Polym. Chem. 5 (2014) 3119–3141.
[8] D. Sun, S. Sato, W. Ueda, A. Primo, H. Garcia, A. Corma, Production of C4 and C5 alcohols from biomass-derived materials, Green Chem. 18 (2016) 2579–2597.
[9] J.S. Luterbacher, D. Martin Alonso, J.A. Dumesic, Targeted chemical upgrading of lignocellulosic biomass to platform molecules, Green Chem. 16 (2014) 4816–4838.

[10] M. Pagliaro, R. Ciriminna, H. Kimura, M. Rossi, C. Della, From glycerol to value-added products, Angew. Chem. Int. Ed. Engl. 46 (2007) 4434–4440.
[11] P. Manjunathan, S.P. Maradur, A.B. Halgeri, G.V. Shanbhag, Room temperature synthesis of solketal from acetalization of glycerol with acetone: effect of crystallite size and the role of acidity of beta zeolite, J. Mol. Catal. A: Chem. 396 (2015) 47–54.
[12] C.H. Zhou, J.N. Beltramini, Y.X. Fan, G.Q. Lu, Chemoselective catalytic conversion of glycerol as a biorenewable source to valuable commodity chemicals, Chem. Soc. Rev. 37 (2008) 527–549.
[13] J.C. Yori, S.A. D'Ippolito, C.L. Pieck, C.R. Vera, Deglycerolization of biodiesel streams by adsorption over silica beds, Energy Fuels 21 (2007) 347–353.
[14] L. Bournay, D. Casanave, B. Delfort, G. Hillion, J.A. Chodorge, New heterogeneous process for biodiesel production: a way to improve the quality and the value of the crude glycerin produced by biodiesel plants, Catal. Today 106 (2005) 190–192.
[15] F.H. Isikgor, C.R. Becer, Lignocellulosic biomass: a sustainable platform for the production of bio-based chemicals and polymers, Polym. Chem. 6 (2015) 4497–4559.
[16] P. Gallezot, Conversion of biomass to selected chemical products, Chem. Soc. Rev. 41 (2012) 1538–1558.
[17] J.J. Bozell, G.R. Petersen, Technology development for the production of biobased products from biorefinery carbohydrates—the US Department of Energy's "Top 10" revisited, Green Chem. 12 (2010) 539–554.
[18] R. Christoph, B. Schmidt, U. Steinberner, W. Dilla, R. Karinen, Ullmann's Encycl. Ind. Chem. 16 (1998) 67–82.
[19] J. Lange, J. Rieumont, N. Davidenko, R. Sastre, Photoinitiated bulk polymerization of furfuryl methacrylate. Experimental and kinetic modelling results obtained at different temperatures, Polymer 39 (1998) 2537–2542.
[20] C. Peniche, D. Zaldívar, A. Bulay, J.S. Román, Influence of chain microstructure on thermodegradative behavior of furfuryl methacrylate-N-vinylpyrrolidone random copolymers by thermogravimetry, J. Appl. Polym. Sci. 50 (1993) 2121–2127.
[21] A.A. Kavitha, N.K. Singha, Atom-transfer radical copolymerization of furfuryl methacrylate (FMA) and methyl methacrylate (MMA): a thermally-amendable copolymer, Macromol. Chem. Phys. 208 (2007) 2569–2577.
[22] E. Goiti, F. Heatley, M.B. Huglin, J.M. Rego, Kinetic aspects of the Diels–Alder reaction between poly(styrene-co-furfuryl methacrylate) and bismaleimide, Eur. Polym. J. 40 (2004) 1451–1460.
[23] J.A. Melero, G. Vicente, G. Morales, M. Paniagua, J. Bustamante, Oxygenated compounds derived from glycerol for biodiesel formulation: influence on EN 14214 quality parameters, Fuel 89 (2010) 2011–2018.
[24] S.O. Kyerematen, E. Amado, J. Kressler, Synthesis and characterization of random copolymers of (2,2-dimethyl-1,3-dioxolan-4-yl)methyl methacrylate and 2,3-dihydroxypropyl methacrylate, Eur. Polym. J. 43 (2007) 3380–3391.
[25] R.G.M.R. Barroso, S.B. Gonçalves, F. Machado, A novel approach for the synthesis of lactic acid-based polymers in an aqueous dispersed medium, Sustain. Chem. Pharm. 15 (2020), 100211.
[26] P.S. Moyo, L.C. Matsinha, B.C.E. Makhubela, Pd(II) and Pt(II) catalysed selective synthesis of furfuryl alcohol: solvent effects and insights into the mechanism, J. Organomet. Chem. 922 (2020), 121362.
[27] S. Zaher, L. Christ, M. Abd El Rahim, A. Kanj, I. Karamé, Green acetalization of glycerol and carbonyl catalyzed by FeCl 3·6H_2O, Mol. Catal. 438 (2017) 204–213.
[28] P. Ray, T. Hughes, C. Smith, G.P. Simon, K. Saito, Synthesis of bioacrylic polymers from dihydro-5-hydroxyl furan-2-one (2H-HBO) by free and controlled radical polymerization, ACS Omega 3 (2018) 2040–2048.
[29] P. Ray, T. Hughes, C. Smith, M. Hibbert, K. Saito, G.P. Simon, Development of bio-acrylic polymers from CyreneTM: transforming a green solvent to a green polymer, Polym. Chem. 10 (2019) 3334–3341.
[30] P. Rajalakshmi, J.M. Marie, A.J. Maria Xavier, Castor oil-derived monomer ricinoleic acid based biodegradable unsaturated polyesters, Polym. Degrad. Stab. 170 (2019), 109016.
[31] Á. O'Driscoll, J.J. Leahy, T. Curtin, The influence of metal selection on catalyst activity for the liquid phase hydrogenation of furfural to furfuryl alcohol, Catal. Today 279 (2017) 194–201.
[32] J. Wu, Y. Shen, C. Liu, H. Wang, C. Geng, Z. Zhang, Vapor phase hydrogenation of furfural to furfuryl alcohol over environmentally friendly Cu–Ca/SiO_2 ₑatalyst, Catal. Commun. 6 (2005) 633–637.
[33] P.D. Vaidya, V.V. Mahajani, Kinetics of liquid-phase hydrogenation of furfuraldehyde to furfuryl alcohol over a Pt/C catalyst, Ind. Eng. Chem. Res. 42 (2003) 3881–3885.
[34] J. Kijeński, P. Winiarek, T. Paryjczak, A. Lewicki, A. Mikolajska, Platinum deposited on monolayer supports in selective hydrogenation of furfural to furfuryl alcohol, Appl. Catal. A: Gen. 233 (2002) 171–182.
[35] B.M. Nagaraja, V. Siva Kumar, V. Shasikala, A.H. Padmasri, B. Sreedhar, B. David Raju, K.S. Rama Rao, A highly efficient Cu/MgO catalyst for vapour phase hydrogenation of furfural to furfuryl alcohol, Catal. Commun. 4 (2003) 287–293.
[36] Z. Zhou, Q. Ma, A. Zhang, L. Wu, Scallop phenylalanine hydroxylase implicates in immune response and can be induced by human TNF-α, Fish. Shellfish Immunol. 31 (2011), 856-63.
[37] K. Balani, V. Verma, A. Agarwal, R. Narayan, Biosurfaces (in), John Wiley & Sons, Inc, Hoboken, NJ, USA, 2015, pp. 329–344 (in).
[38] A. Gugliuzza, E. Drioli, PVDF and HYFLON AD membranes: ideal interfaces for contactor applications, J. Membr. Sci. 300 (2007) 51–62.